Making and Breaking Covalent Bonds across the Magnetic Transition in the Giant Magnetocaloric Material $Gd_5(Si_2Ge_2)$

W. Choe,[1] V. K. Pecharsky,[2] A. O. Pecharsky,[2] K. A. Gschneidner, Jr.,[2] V. G. Young, Jr.,[3] and G. J. Miller[1,*]

[1]*Department of Chemistry, Iowa State University, Ames, Iowa 50011*

[2]*Ames Laboratory and Department of Materials Science and Engineering, Iowa State University, Ames, Iowa 50011*

[3]*Department of Chemistry, University of Minnesota, Minneapolis, Minnesota 55455*

(Received 8 November 1999)

A temperature-dependent, single crystal x-ray diffraction study of the giant magnetocaloric material, $Gd_5(Si_2Ge_2)$, across its Curie temperature (276 K) reveals that the simultaneous orthorhombic to monoclinic transition occurs by a shear mechanism in which the (Si, Ge)-(Si, Ge) dimers that are richer in Ge increase their distances by 0.859(3) Å and lead to twinning. The structural transition changes the electronic structure, and provides an atomic-level model for the change in magnetic behavior with temperature in the $Gd_5(Si_xGe_{1-x})_4$.

PACS numbers: 61.50.Ks, 61.66.Dk, 64.70.Kb

The recently discovered $Gd_5(Si_2Ge_2)$ and related $Gd_5(Si_xGe_{1-x})_4$ phases, where $x \leq 0.5$, exhibit a giant magnetocaloric effect close to 300 K due to a first order magnetic phase transition [1–3], making $Gd_5(Si_2Ge_2)$ a promising candidate for near room temperature magnetic refrigeration [4,5]. Further developments in new magnetic refrigerants and magnetic refrigeration technology could lead to the replacement of current vapor-cycle refrigerators with more energy efficient and environmentally benign devices. A complete understanding of the nature of the giant magnetocaloric effect in $Gd_5(Si_2Ge_2)$ is, therefore, of fundamental and practical importance towards the design of even better magnetic refrigerant materials. $Gd_5(Si_2Ge_2)$ belongs to the family of compounds $Gd_5(Si_xGe_{1-x})_4$, which shows variation in Curie temperature and room temperature crystal structure with composition [6]. A recent study [7] showed that a ferromagnetic (low temperature) to paramagnetic (high temperature) magnetic phase transition in $Gd_5(Si_{1.8}Ge_{2.2})$ occurs simultaneously with an orthorhombic (low temperature) to monoclinic (room temperature) crystallographic phase transformation, according to x-ray powder diffraction. However, important structural details concerning the distribution of Si and Ge, as well as changes in bond distances and local coordination environments remain unresolved. This Letter describes the first temperature-dependent, single-crystal, atomic-scale, structural study of $Gd_5(Si_2Ge_2)$ across its magnetic phase transition, and reveals a simultaneous crystallographic (orthorhombic/monoclinic) transition that involves breaking and forming covalent bonds between Si and Ge atoms. Such solid-solid, first order phase transitions typically occur with changes in much weaker interactions such as hydrogen bonding [8,9], or van der Waals forces [10], because changes in covalent bonding [11] often lead to the irreversible formation of a new phase [12]. The effect of this extraordinary phenomenon on the electronic structure of $Gd_5(Si_2Ge_2)$ and on the exchange interaction between Gd atoms is also addressed.

The $Gd_5(Si_2Ge_2)$ alloy was prepared by arc melting [6], followed by 1 h heat treatment at 1570 K. X-ray diffraction data were collected at temperatures 163, 243, and 292 K, using a Bruker CCD-1000, three-circle diffractometer with Mo K_α radiation on a single crystal with dimensions $0.1 \times 0.1 \times 0.2$ mm^3 extracted from this alloy. Structure solutions and refinements were performed with SHELXTL. The structure of $Gd_5(Si_2Ge_2)$ at 163 and 243 K (called the α phase hereafter) is orthorhombic, crystallizes in space group *Pnma* (No. 62), which agrees with Ref. [7], and belongs to the Gd_5Si_4 structure type [13] (see Tables I and II). Figure 1(a) shows two projections of α-$Gd_5(Si_2Ge_2)$: (top) Along the **b** axis; and (bottom) along the **c** axis. Gd atoms form quasi-infinite, two-dimensional (3^2434) nets. Two adjacent Gd (3^2434) nets create a slab composed of distorted cubes and trigonal prisms sharing common faces. A *nonstatistical* mixture of Si and Ge atoms (green, ca. 60% Si and 40% Ge), called "*T*" atoms hereafter, occupy the trigonal prisms in these slabs, which share a common rectangular face to create T_2 dimers (T-T distance is ca. 2.56 Å). The Gd atom in the center of each cube (blue) is surrounded by an octahedral arrangement of four T atoms and two T' atoms (red; T' represents another mixture of Ge and Si atoms, ca. 40% Si and 60% Ge). As seen along the **c** direction in Fig. 1(a), each (3^2434) slab is connected to two adjacent slabs by T'-T' bonds (ca. 2.62 Å). Therefore,

TABLE I. Crystallographic data for $Gd_5(Si_2Ge_2)$.

Temperature	163 K	243 K	292 K
Space group	*Pnma*	*Pnma*	$P112_1/a$
a, Å	7.5137(11)	7.5132(11)	7.5891(17)
b, Å	14.792(2)	14.797(2)	14.827(3)
c, Å	7.7858(11)	7.7942(11)	7.7862(17)
γ, deg	90	90	93.262(4)
V, Å^3	865.3(2)	866.5(2)	874.7(3)
R_1 ($F_0 > 4\sigma$)	0.0273	0.0274	0.0416

TABLE II. Atomic positions and equivalent thermal displacement parameters[a] in the crystal structures of $Gd_5(Si_2Ge_2)$ at 243 and 292 K.

243 K	x/a	y/b	z/c	Occupancy[b]	U_{eq}, Å^2
Gd1	0.022 96(7)	0.403 18(3)	0.182 32(6)	1	0.006 85(18)
Gd2	0.679 62(6)	0.377 32(3)	0.822 55(6)	1	0.005 60(18)
Gd3	0.149 58(9)	0.75	0.510 11(8)	1	0.0057(2)
$T1$ (T')	0.846 89(18)	0.459 84(9)	0.529 29(18)	0.574(5) Ge	0.0072(5)
$T2$ (T)	0.0235(3)	0.75	0.1021(3)	0.390(6) Ge	0.0063(8)
$T3$ (T)	0.2681(3)	0.75	0.8711(3)	0.443(6) Ge	0.0058(7)
292 K					
Gd1A	0.017 31(11)	0.401 00(6)	0.182 03(11)	1	0.0077(2)
Gd1B	0.005 15(11)	0.901 65(6)	0.819 42(11)	1	0.0075(2)
Gd2A	0.669 97(11)	0.377 95(5)	0.822 56(11)	1	0.0060(2)
Gd2B	0.356 60(10)	0.881 36(6)	0.163 28(11)	1	0.0064(2)
Gd3	0.175 34(11)	0.753 55(6)	0.505 62(11)	1	0.0064(2)
$T1A$ (T')	0.8460(3)	0.458 98(16)	0.5294(3)	0.575(7) Ge	0.0083(8)
$T1B$ (T')	0.2068(3)	0.957 94(17)	0.4639(3)	0.570(8) Ge	0.0083(8)
$T2$ (T)	0.0477(3)	0.7483(2)	0.1082(4)	0.429(7) Ge	0.0090(9)
$T3$ (T)	0.2913(3)	0.747 93(19)	0.8691(4)	0.461(7) Ge	0.0074(8)

[a]All crystallographic parameters can be received from the authors upon request.
[b]All T and T' sites are fully occupied with Si and Ge atoms. In this table only Ge occupations are listed.

in α-$Gd_5(Si_2Ge_2)$, all Si and Ge atoms are involved in dimers.

The room temperature form of $Gd_5(Si_2Ge_2)$ [β phase, shown in Fig. 1(b)] crystallizes in the monoclinic space group $P112_1/a$ (No. 14) (see Tables I and II), and involves nearly identical (3^2434) slabs seen in the α phase, with one-half of the T'-T' bonds (the $T1B$-$T1B$ bonds, Table II) connecting these slabs "broken," their $T1B$-$T1B$ distance expands by 32.7% from 2.629(3) Å (α phase at 243 K) to 3.488(3) Å (β phase at 292 K). Note this effect occurs in the Ge-rich dimers. The short $T1A$-$T1A$ distance remains at 2.614(3) Å. This drastic structural change arises from a large shear movement of pairs of (3^2434) slabs in the α phase by ca. 0.8 Å along the $+\mathbf{a}$ or $-\mathbf{a}$ direction relative to one another [see arrows in Fig. 1(a)]. Within a pair of adjacent slabs maintaining the T'-T' connection, interatomic distances change less than 3% during the $\alpha \leftrightarrow \beta$ transformation. Despite the shear nature of the transition, our repeated temperature-dependent x-ray diffraction experiments confirm that this transformation is reproducible on heating and cooling. Furthermore, the magnetic and heat capacity data for $Gd_5(Si_2Ge_2)$ [1] indicate that the $\alpha \leftrightarrow \beta$ transformation can be induced by a changing magnetic field, as was reported for $Gd_5(Si_{1.8}Ge_{2.2})$ [7]. When the field is applied to a β phase at temperatures just exceeding 276 K, the paramagnetic β phase transforms to the ferromagnetic α phase. Reducing the magnetic field to 0 T at constant temperature creates the paramagnetic β phase from the ferromagnetic α phase. Therefore, this structural transition is controlled by composition [6], temperature, and magnetic field [1–3,7].

As the $\alpha \leftrightarrow \beta$ transition occurs, the crystals show macroscopic twinning, which was first indicated by significant residual electron densities (ca. 7.9 $e^-/$Å^3) in the fully refined, initial β-phase model. No such residual electron densities were seen in the α-phase model. These electron density residues reveal an additional (3^2434) net next to the Gd (3^2434) net already present in the refined β-phase model, and suggest our initial structure model is incomplete. Subsequent examination of the charge-coupled device frame data for the β phase showed a considerable number of reflections with noninteger indices along only the $\mathbf{b}^*$ axis and all multiples of $\frac{1}{9}$ ($k = 0.1111, 0.2222, 0.3333$, etc.). Two possibilities can account for this phenomenon: the formation of a ninefold superstructure along the **b** axis or nonmerohedral twinning [14,15]. For a superstructure, all reflections would occur from a single individual crystal. On the other hand, nonmerohedral twinning in a crystal produces a diffraction pattern in which only a small fraction of reflections from two macroscopic components are exactly superimposed, while the majority of the reflections from each individual remain separate. We found that nonmerohedral twinning is responsible, since we could generate a relationship (a matrix transformation called the twin law) between twinned individuals and achieve significant improvement in the statistical fit of observed and calculated structure factors. This phenomenon is also coupled to the crystallographic changes: twinning vanishes when the crystal is cooled below ca. 260 K as the α phase forms, and it reappears on heating to room temperature as the β phase forms. All of the single crystalline specimens ($\sim$20) examined were nonmerohedral twins at room temperature, suggesting that twinning is an intrinsic feature of the monoclinic β phase.

Breaking one-half of the T'-T' dimers, together with the shear movement of the (3^2434) slabs along the **a** axis,

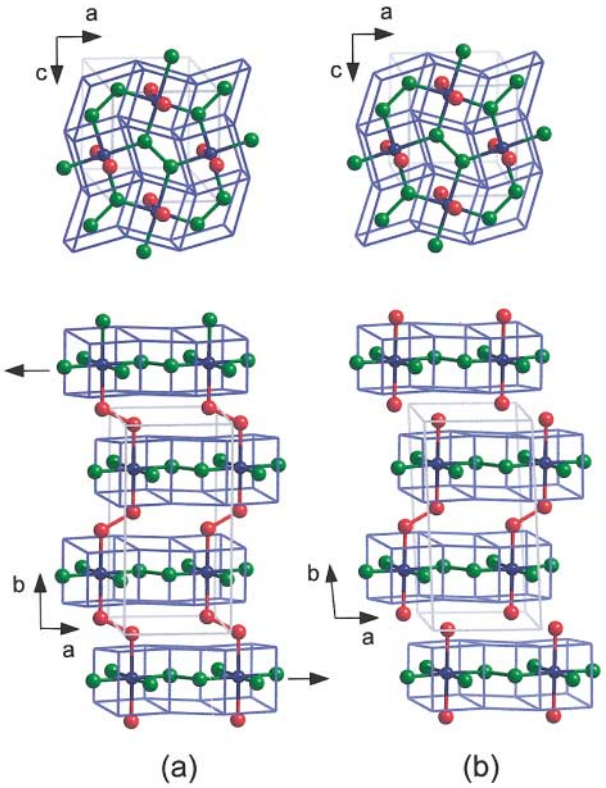

FIG. 1 (color). The crystal structures of (a) orthorhombic α- and (b) monoclinic β-$Gd_5(Si_2Ge_2)$ shown along the **b** (top) and **c** axes (bottom). The **b** axis projections emphasize the Gd (3^2434) nets with Gd in cubic and T atoms (Si or Ge) in trigonal prismatic holes. The **c** projections show the T' atoms (Si or Ge) in red and emphasize that one-half of these dimers are broken in the β phase. The arrows indicate the shift of (3^2434) slabs from the α to the β phase.

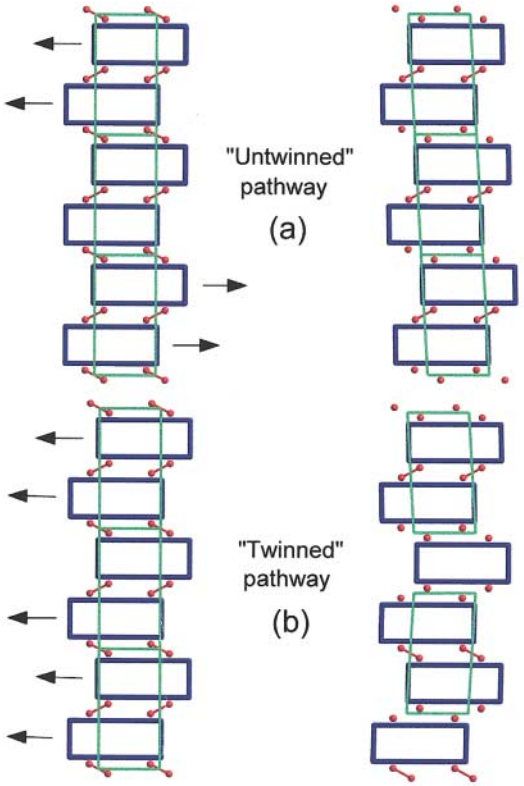

FIG. 2 (color). Two possible pathways for the $\alpha \leftrightarrow \beta$ structure transformation by shear movement along the **a** axis. The arrows indicate the direction in which slab movement occurs in α-$Gd_5(Si_2Ge_2)$ assuming the "untwinned" (a) or a "twinned" (b) pathway for the formation of β-$Gd_5(Si_2Ge_2)$. The two figures on the left represent the crystal structure of the α phase while the two on the right show an untwinned (top) and a twinned (bottom) model for monoclinic β-$Gd_5(Si_2Ge_2)$.

explains the nature of the $\alpha \leftrightarrow \beta$ phase transformation, as well as the twinning observed in the β phase. Figure 2 illustrates a model of the possible twin mechanism during the phase transition. For no twinning in the β phase, alternating layers of T'-T' dimers are broken as adjacent pairs of slabs shift in opposite directions along the **a** axis [see the arrows in Fig. 2(a)]. On the other hand, if two adjacent layers of T'-T' dimers are broken, then two different orientations of equivalent monoclinic unit cells are generated, which are related to each other by a mirror operation in the **ac** plane [perpendicular to the $\mathbf{b}^*$ axis; see Fig. 2(b)], and nonmerohedral twinning occurs.

The β phase is a 1:1 intergrowth between the Gd_5Si_4 type [13], as in α-$Gd_5(Si_2Ge_2)$, and the Sm_5Ge_4 type [16], as in Gd_5Ge_4. In this series, the number of T-T dimers per formula unit changes with the crystal structure type. The low-temperature α phase contains two T_2 dimers/formula unit. According to the Zintl-Klemn formalism [17], formal charges for isolated T atoms and T_2 dimers are -4 and -6 to satisfy closed shell configurations for Si or Ge, assuming a single bond in each T-T dimer. The corresponding charge balanced formula is $[(Gd^{3+})_5(T_2^{6-})_2(3e^-)]$, which indicates three electrons assigned to the conduction band. In the same way, β-$Gd_5(Si_2Ge_2)$ has 1.5 T_2 dimers and 1 T monomer/formula unit, $[(Gd^{3+})_5(T_2^{6-})_{1.5}(T^{4-})(2e^-)]$, and the binary compound Gd_5Ge_4, or a hypothetical "γ-$Gd_5(Si_2Ge_2)$," contains 1 T_2 dimer and 2 T monomers/formula unit, $[(Gd^{3+})_5(T_2^{6-})(T^{4-})_2(1e^-)]$. The decrease in both the number of dimers as well as electrons available for metallic bonding in the conduction band certainly affects the electronic structure and magnetic properties of $Gd_5(Si_2Ge_2)$. Preliminary tight binding calculations show that the σ_p^* orbital of the T'-T' dimers is located just above the Fermi level in the total density of states of $Gd_5(Si_2Ge_2)$ and remains unoccupied at low temperatures. The σ_p^* orbital of the T-T dimers is much higher in energy, due to the greater concentration of Si atoms on the T sites in $Gd_5(Si_2Ge_2)$ than on the T' sites (see Table II): Ge is more electronegative than Si, so the energies of Ge orbitals are lower than the energies of Si orbitals [18]. Raising the temperature will promote electron transfer from states just below the Fermi level in the T'-T' σ_p^* states, drive the breaking of just these bonds in α-$Gd_5(Si_2Ge_2)$, and play a crucial role in the $\alpha \leftrightarrow \beta$ phase transition as well as the twinning process.

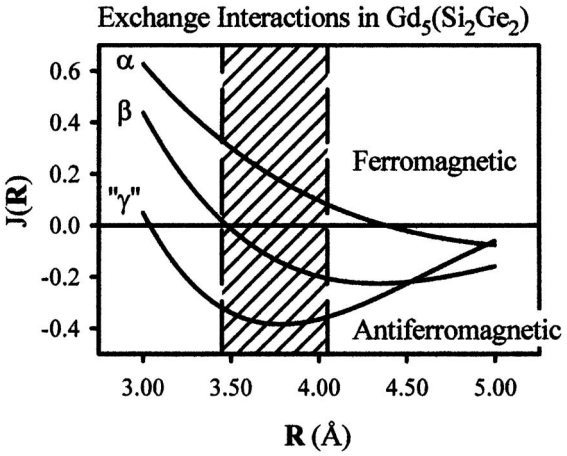

FIG. 3. Variations in the exchange interactions, $J(\mathbf{R})$, between Gd atoms in $Gd_5(Si_2Ge_2)$ with Gd-Gd distance, $\mathbf{R}$ as estimated from the RKKY model using a nearly free electron model for the conduction electrons. The hatched region between 3.45 and 4.05 Å corresponds to the range of short Gd-Gd contacts.

The covalent bond breaking/forming mechanism of the $\alpha \leftrightarrow \beta$ transformations also enables a qualitative understanding of the existence of the giant magnetocaloric effect in $Gd_5(Si_2Ge_2)$. As the temperature drops below the Curie point, T'-T' dimer formation in the α phase, together with the increase in valence electron concentration available for metallic bonding, sharply enhances the exchange interactions between Gd atoms and causes the material to order ferromagnetically. Using a nearly free electron model for the conduction band and applying the RKKY model [19] to calculate the effective exchange parameter $J(\mathbf{R})$ between Gd sites in the α and β phases confirms this change (see Fig. 3). From β- to α-$Gd_5(Si_2Ge_2)$, Gd-Gd distances do not change [they range from 3.436(1) to 4.053(1) Å], so the sign of the exchange interaction depends on k_F, which is proportional to $(\text{valence}/\text{volume})^{1/3}$. As shown above, the valence increases from β- to α-$Gd_5(Si_2Ge_2)$ and the volume decreases. Therefore, in β-$Gd_5(Si_2Ge_2)$, $J(\mathbf{R}) > 0$ for short Gd-Gd contacts and $J(\mathbf{R}) < 0$ for long Gd-Gd contacts. On the other hand, in α-$Gd_5(Si_2Ge_2)$, $J(\mathbf{R}) > 0$ for the entire range of Gd-Gd interactions (hatched region in Fig. 3). Therefore, the significant changes in electronic structure as $Gd_5(Si_2Ge_2)$ undergoes the $\alpha \leftrightarrow \beta$ transformation also affect the exchange interactions. Furthermore, the atomic scale, structural detail provided by this study account for the narrow temperature range over which the first order transition occurs, which leads to a large $|\partial M/\partial T|$ and, consequently, to a giant magnetocaloric effect [1,2,20]. Further theoretical and experimental investigations are currently underway to investigate these phenomena.

This work was supported by the Materials Sciences Division, Office of Basic Energy Sciences, U.S. Department of Energy (V. K. P., K. A. G., and A. O. P.) under W-7405-ENG-82, and the NSF (W. C., G. J. M., and V. G. Y.) under DMR-96-27161.

*Electronic address: gmiller@iastate.edu.

[1] V. K. Pecharsky and K. A. Gschneidner, Jr., Phys. Rev. Lett. **78**, 4494–4497 (1997).
[2] V. K. Pecharsky and K. A. Gschneidner, Jr., Appl. Phys. Lett. **70**, 3299–3301 (1997).
[3] V. K. Pecharsky and K. A. Gschneidner, Jr., J. Magn. Magn. Mater. **167**, L179–L184 (1997).
[4] C. B. Zimm, Adv. Cryog. Eng. **43**, 1759–1766 (1998).
[5] V. K. Pecharsky and K. A. Gschneidner, Jr., J. Magn. Magn. Mater. **200**, 44 (1999).
[6] V. K. Pecharsky and K. A. Gschneidner, Jr., J. Alloys Compd. **260**, 98–106 (1997).
[7] L. Morellon *et al.*, Phys. Rev. B **58**, R14 721 (1998).
[8] M. T. Reetz, S. Hoeger, and K. Harms, Angew. Chem., Int. Ed. Engl. **33**, 181–183 (1994).
[9] A. M. Dattelbaum and J. D. Martin, Inorg. Chem. **38**, 2369–2374 (1999).
[10] R. Boese, T. Miebach, and A. De Meijere, J. Am. Chem. Soc. **113**, 1743–1748 (1991).
[11] P. W. Stephens *et al.*, Nature (London) **370**, 636–639 (1994).
[12] N. Sidorov *et al.*, Ferroelectrics **114**, 223–230 (1993).
[13] G. S. Smith, Q. Johnson, and A. G. Tharp, Acta Crystallogr. **22**, 940–943 (1967).
[14] R. Herbst-Irmer and G. M. Sheldrick, Acta Crystallogr. B **54**, 443 (1998).
[15] G. J. Miller and J. Lin, Angew. Chem., Int. Ed. Engl. **33**, 334–336 (1994).
[16] F. Holtzberg, R. J. Gambino, and T. R. McGuire, J. Phys. Chem. Solids **28**, 2283–2289 (1967).
[17] G. J. Miller, in *Chemistry, Structure, and Bonding of Zintl Phases and Ions*, edited by S. M. Kauzlarich (VCH Publishers, New York, 1996), pp. 1–59.
[18] G. J. Miller, Eur. J. Inorg. Chem. 528–536 (1998).
[19] J. Callaway, *Quantum Theory of the Solid State* (Academic Press, New York, 1991), 2nd ed.
[20] A. Giguère *et al.*, Phys. Rev. Lett. **83**, 2262 (1999).